

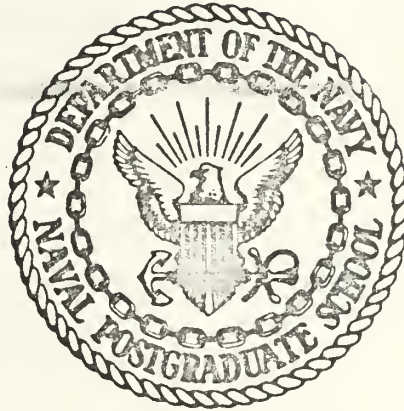
HIGH-TEMPERATURE TEXTURE STRENGTHENING
IN α -TITANIUM

Robert William Rolfes

NOX LIBRARY
POSTGRADUATE SCHOOL
PASADENA, CALIFORNIA 93940

NAVAL POSTGRADUATE SCHOOL

Monterey, California



THESIS

HIGH-TEMPERATURE TEXTURE STRENGTHENING
IN α -TITANIUM

by

Robert William Rolfes

June 1974

Thesis Advisor:

Glen Edwards

Approved for public release; distribution unlimited.

T16178

REPORT DOCUMENTATION PAGE		READ INSTRUCTIONS BEFORE COMPLETING FORM
1. REPORT NUMBER	2. GOVT ACCESSION NO.	3. RECIPIENT'S CATALOG NUMBER
4. TITLE (and Subtitle) High-Temperature Texture Strengthening In α -Titanium		5. TYPE OF REPORT & PERIOD COVERED Master's Thesis June 1974
7. AUTHOR(s) Robert William Rolfes		6. PERFORMING ORG. REPORT NUMBER
9. PERFORMING ORGANIZATION NAME AND ADDRESS Naval Postgraduate School Monterey, California 93940		8. CONTRACT OR GRANT NUMBER(s)
11. CONTROLLING OFFICE NAME AND ADDRESS Naval Postgraduate School Monterey, California 93940		10. PROGRAM ELEMENT, PROJECT, TASK AREA & WORK UNIT NUMBERS
14. MONITORING AGENCY NAME & ADDRESS (If different from Controlling Office) Naval Postgraduate School Monterey, California 93940		12. REPORT DATE June 1974
		13. NUMBER OF PAGES 51
		15. SECURITY CLASS. (of this report) Unclassified
		15a. DECLASSIFICATION/DOWNGRADING SCHEDULE
16. DISTRIBUTION STATEMENT (of this Report) Approved for public release; distribution unlimited.		
17. DISTRIBUTION STATEMENT (of the abstract entered in Block 20, if different from Report)		
18. SUPPLEMENTARY NOTES		
19. KEY WORDS (Continue on reverse side if necessary and identify by block number)		
20. ABSTRACT (Continue on reverse side if necessary and identify by block number) The high-temperature texture strengthening behavior of α -titanium has been investigated over a wide range of temperatures (.30 to .55T _m) and strain rates (1.66×10^{-2} to 1.54×10^{-5} sec ⁻¹). The activation energy for creep, Q _c , was found to be 80% higher than the accepted value for self-diffusion, Q _{sd} . Cross-rolling samples with a subsequent anneal produced a strong duplex texture. Textured transverse samples were consistently stronger than longitudinal samples with a 40% difference in strength at the lowest creep rates and in the temperature range most useful for titanium (300-500°C).		

High-Temperature Texture Strengthening
in α -Titanium

by

Robert William Rolfes
Ensign, United States Navy
B.S. United States Naval Academy, 1973

Submitted in partial fulfillment of the
requirements for the degree of

MASTER OF SCIENCE IN MECHANICAL ENGINEERING

from the

NAVAL POSTGRADUATE SCHOOL

June 1974

Thesis
R68946

ABSTRACT

The high-temperature texture strengthening behavior of α -titanium has been investigated over a wide range of temperatures (.30 to .55T_m) and strain rates (1.66×10^{-2} to $1.54 \times 10^{-5} \text{ sec}^{-1}$). The activation energy for creep, Q_c , was found to be 80 percent higher than the accepted value for self-diffusion, Q_{sd} . Cross-rolling samples with a subsequent anneal produced a strong duplex texture. Textured transverse samples were consistently stronger than longitudinal samples, with a 40 percent difference in strength at the lowest creep rates and in the temperature range most useful for titanium (300 - 500°C).

TABLE OF CONTENTS

List of Tables	6
List of Illustrations	7
I. INTRODUCTION	10
A. TECHNOLOGICAL NEED FOR TITANIUM	10
B. PREFERRED ORIENTATION	11
C. PLASTIC DEFORMATION IN THE HCP CRYSTAL STRUCTURE	13
D. RECRYSTALLIZATION TEXTURES IN HCP METALS	15
II. NATURE OF INVESTIGATION	16
A. INVESTIGATION OF HIGH TEMPERATURE DEFORMATION OF PURE α -TITANIUM	16
B. INVESTIGATION OF HIGH TEMPERATURE TEXTURE STRENGTHENING IN α -TITANIUM	17
III. EXPERIMENTAL PROCEDURE	19
A. EQUIPMENT DESCRIPTION AND SAMPLE PREPARATION	19
B. TEST PROCEDURE	21
C. METHOD OF DATA TAKING	22
D. TEXTURE EVALUATION	22
1. X-ray Diffraction	22
2. Texture Determined by Polarized Light Microscopy	23
E. DATA ANALYSIS	24
IV. RESULTS AND DISCUSSION	25
A. CREEP BEHAVIOR OF α -TITANIUM	25
B. TEXTURE ANALYSIS	26
C. TEXTURE STRENGTHENING	28
V. CONCLUSIONS	30
References	50
Initial Distribution List	52

LIST OF TABLES

I	Chemical Composition of Titanium used in the Investigation.	31
II	Matrix of Temperatures and Cross-Head Speeds used for tests.	32

LIST OF FIGURES

1.	HCP Unit cell with principal planes and directions indicated.	33
2.	Comparison of activation energies for creep and self diffusion for various materials.	33
3.	Ideal recrystallization texture in titanium sheet; Basal [0001] poles are perpendicular to R.D. and the [10 $\bar{1}$ 0] direction is parallel to R.D.	34
4.	Ideal duplex recrystallization texture in cross-rolled and annealed α -titanium. Equal numbers of grains occupy each of the orientations depicted.	35
5.	Instron Model TT-D testing machine with compression rig.	36
6.	Compression rig with Marshall Furnace.	37
7.	Synchronous motor on Instron machine; Used for slowest strain rate.	38
8.	Longitudinal and transverse samples sectioned from cross-rolled bar.	39
9.	View of grain structure of textured sample 100X.	39
10.	X-ray diffraction pattern obtained from titanium filings.	40
11.	Plot of strain rate versus normalized flow stress at constant temperature; Longitudinal samples of cross-rolled α -titanium.	41
12.	Plot of strain rate versus normalized flow stress at constant temperature; Transverse samples of cross-rolled α -titanium.	42
13.	Plot of strain rate versus inverse of temperature at constant σ/E .	43
14.	X-ray diffraction pattern obtained from textured titanium sample.	44
15.	Photo-micrograph of textured α -titanium sample under polarized light; Plane view is perpendicular to R.D. (a) grains in original orientation, (b) grains after 90° rotation.	45

16. Plot of flow stress at 10 percent strain versus temperature for textured α -titanium; $\dot{\epsilon} = 1.66 \times 10^{-2} \text{ sec}^{-1}$. 46
17. Plot of flow stress at 10 percent strain versus temperature for textured α -titanium; $\dot{\epsilon} = 1.66 \times 10^{-3} \text{ sec}^{-1}$. 47
18. Plot of flow stress at 10 percent strain versus temperature for textured α -titanium; $\dot{\epsilon} = 1.66 \times 10^{-4} \text{ sec}^{-1}$. 48
19. Plot of flow stress at 10 percent strain versus temperature for textured α -titanium; $\dot{\epsilon} = 1.54 \times 10^{-5} \text{ sec}^{-1}$. 49

ACKNOWLEDGEMENTS

I am especially indebted to my advisor, Professor Glen R. Edwards for his excellent guidance and professional demeanor. His ability to steer me on a course and keep me out of the fog has made this research a very fulfilling experience. I am also grateful to Mr. Roy Edwards, whose ingenuity and resourcefulness makes the Material Science group go.

I am most thankful to Miss Karen Lee Estill whose motivation and inspiration kept the project moving when things got slow.

I. INTRODUCTION

A. TECHNOLOGICAL NEED FOR TITANIUM

In recent times the development of the hydrofoil has called for the design of high strength low weight struts. The accelerated development of high-performance jet aircraft has called for a new emphasis on structural designs utilizing strong tough materials which are inherently light. Both the materials selection examples cited above emphasize the growing need for titanium-base alloys, which are particularly desirable because of their high strength-to-weight ratio. Attention is focused upon titanium because of its superior strength-to-density ratio over a wide range of temperatures (-198°C to over 600°C) as compared to such structural materials as aluminum alloys and steels. Titanium alloys in the past twenty years have played an important part in structural design, especially the design of aircraft parts. Alloys such as Ti-6Al/4V have been extensively used in gas turbine engine compressor sections for over ten years [1].

The trend in aircraft design has consistently been toward faster speeds, higher payloads and greater overall performance. This means higher room and elevated temperature strength requirements for structural parts which must be as light as possible.

Even though titanium has the properties that will meet most of the needs cited above, some problems do exist. Oxidation embrittlement causes a serious loss in ductility and fatigue strength. Internal microstructural instabilities occur in all of the stronger titanium alloys presently available, which cause large strength and ductility losses in long times under stress above $500 - 550^{\circ}\text{C}$, [2]. Between the surface instabilities and the microstructural instabilities, titanium has problems in its use above 500°C .

Obviously, there exists the need to improve the elevated temperature properties of titanium alloys. A first step towards improving the elevated temperature properties of titanium alloys is a thorough understanding of high-temperature behavior of the pure metal.

B. PREFERRED ORIENTATION

The metallurgical term "preferred orientation" is used to describe a polycrystalline material in which many of the individual grains possess the same crystallographic orientation in space. Because most properties of crystalline solids are structure-sensitive, materials possessing "preferred orientation" or "texture" often manifest anisotropic properties, i.e. different properties in different directions. As an example, consider the development of the Alnico V magnet alloys. It was found that great improvements could be obtained by heat treating certain of these alloys in a strong magnetic field. After processing, the material exhibits excellent magnetic properties, (magnetic energy and useful flux) parallel to the direction of the magnetic field but rather poor magnetic properties in other directions. The improvements in magnetic properties in specific directions can be directly correlated to the degree of "preferred orientation" or "crystallographic texture" created by heat treatment.

Just as it is possible to improve magnetic properties by consideration of the anisotropic properties of Alnico V, it is possible to consider the utilization of crystallographic anisotropy to improve material strength. Ordinary alloys can usually be treated as isotropic (rather than anisotropic as in single crystal). All common structural alloys are polycrystalline, that is they are made up of many very small grains or crystals. If the crystals are randomly oriented, the average

properties will be the same in all directions. But if, as a result of casting, rolling, or heat treating, the grains in a polycrystalline bar may assume very nearly identical orientations, the bar is said to be "textured" and to have a "preferred orientation" which may make its mechanical properties quite directional. As an example, a suitable preferred orientation can greatly increase the stiffness of an iron bar. Assume that the body-centered cubic grains in a pure iron bar all have their [111] directions (body diagonals of the BCC unit cell) aligned parallel to an axis of loading. For a stress of 100 MPa, the strain in an isotropic specimen would be 0.05 percent. For the same stress, the strain in the textured specimen would be only 0.035 percent.

Textured strengthening in alloys has been used for years to improve static mechanical properties of certain alloys at ambient temperatures. As an example of texture strengthening, the work of Vorobév, Gorin, and Khoroshun, [3] indicated the presence of texture created a sharp anisotropy in the wear characteristics of metals. This anisotropy was due to the more favorable disposition of certain slip systems relative to the direction of the friction force. But texture strengthening thus far has not been applied to high-temperature deformation.

Aside from the technological practicability of investigating the effect of texture on the titanium creep strength, there is much to be done in this area to improve the fundamental understanding of high-temperature deformation. Nothing in the generally accepted creep theories takes into account crystallographic texture or mechanical anisotropy.

To better understand how crystallographic anisotropy may occur in α -titanium, a discussion of plastic deformation in the HCP crystal structure is in order.

C. PLASTIC DEFORMATION IN THE HCP CRYSTAL STRUCTURE

On the atomic scale, plastic deformation occurs by slip, or the shearing of the crystal lattice along specific crystallographic planes and directions by the motion of line imperfections called dislocations. Metallurgists have concluded that slip generally occurs most readily on the densely packed but widely spaced planes, and in directions of high atomic density. In other words, dislocations in a particular crystal structure are restricted to move only on discrete planes and in discrete directions; each crystal structure has a limited number of slip systems by which plastic deformation can occur.

Slip systems can operate only if their resolved shear stresses exceed a specific value, the critical resolved shear stress. A shear stress does not exist if the slip plane or the slip direction is perpendicular or parallel to the stress axis. The greatest shear stress occurs when both the slip plane and slip direction are at 45° to the stress axis. Slip occurs when the critical shear stress, τ_c is exceeded, or when:

$$\pm \tau_c = \sigma \cos \lambda \cos \phi . \quad (1)$$

This is known as Schmid's law, where σ is the applied stress, λ is the angle between the slip direction and the stress axis, ϕ is the angle between the normal to the slip plane and the stress axis.

In HCP metals, the unit cell demensions are not always the ideal values implied by the conventional "hard sphere" model of the crystal structure. See Figure 1. If the atoms of HCP metals were all ideally close-packed, the c/a ratio would be the same in all cases (1.633). But it is not the same, and varies from 1.886 for cadmium to 1.586 for

beryllium. Cadmium and zinc have basal-plane separation greater than that of ideally packed spheres, while beryllium, titanium, and zirconium have smaller ones. It is significant that the hexagonal metals with small separations between basal planes are those with very high critical resolved shear stress for basal slip.

HCP metals like cadmium and zinc, with large basal plane separation, have low critical resolved shear stresses on the basal plane. Plastic deformation occurs predominantly by basal slip in these HCP metals.

The transition temperature for titanium is 882°C . Below this temperature the HCP α -phase exists, with a c/a ratio of 1.587 which is about 2 percent less than the "ideal" value of 1.633. Plastic deformation of HCP α -titanium can occur by both dislocation motion or by twinning (a deformation process involving a homogeneous shear strain). The primary direction for all common titanium slip systems is the $\langle 11\bar{2}0 \rangle$ close packed direction. (See Figure 1)

Slip in α -titanium can occur on any of three slip planes, the $(10\bar{1}0)$ and $(10\bar{1}1)$ planes as well as the (0001) basal plane. Because titanium has a c/a ratio below the ideal which results in a high critical shearing stress required for basal slip, slip on the prismatic plane $\{10\bar{1}0\}$ predominates at the temperature of this study.

At high temperatures, slip is by far the predominant deformation process but minor amounts of twinning may persist up to 700°C . [Twinning can be the predominant mode of deformation for low temperatures ($T \leq 200^{\circ}\text{C}$), but will be considered negligible for the range of testing in this study].

D. RECRYSTALLIZATION TEXTURES IN HCP METALS

There are technological ways to produce strong preferred orientations. Invariably these processes involve cold-working by rolling, swaging, or drawing followed by subsequent recrystallization.

For this work, cross-rolling and subsequent recrystallization was used to produce a strong texture with the majority of all the basal poles aligned perpendicular to the rolling direction.

II. NATURE OF INVESTIGATION

A. INVESTIGATION OF HIGH TEMPERATURE DEFORMATION OF PURE α -TITANIUM

The activation energy for creep has been determined for a large number of solids. In Figure 2, this quantity is compared with the activation energy of self-diffusion for several materials. Figure 2 shows that there exists an excellent correlation between the activation energy for creep and the activation energy for self-diffusion. Researchers have obtained Q_{sd} values for α -titanium ranging from 123 kJ/mole to 299 kJ/mole [4].

The work of Dymant and Libanati [5], has concluded that the activation energy for self-diffusion in α -titanium is 150 kJ/mole. This value would appear to be closest to that expected, based on the known self-diffusivity of other similar metals. Following the trend of Figure 2, expected values of the activation energy for creep would be about 150 kJ/mole.

The work of Doner and Conrad [4], in their investigation of the deformation mechanisms in Commercial Ti-50A at intermediate and high temperatures, calculated the activation energy for creep to be 242 kJ/mole, a value seemingly too large to fit the correlation expressed by Figure 2.

The work of Edwards, McNelley, and Sherby [6], in their investigation of high temperature texture strengthening in zinc, showed that this HCP metal was mechanically anisotropic over a wide range of temperatures, but did not attempt to isolate the material property creating the effect.

The purpose of this study was to investigate the creep behavior of α -titanium for the following:

1. To investigate the anomalous behavior reported in the literature pertaining to very high activation energy for titanium creep.

2. To empirically evaluate the mechanical anisotropy in α -titanium creep samples possessing a strong texture. Such an effect would contribute to the state-of-the-art knowledge of titanium behavior, and be useful to designers.

3. To relate the α -titanium creep data to the results obtained for zinc, and thereby help to explain the texture contribution to the basic creep theory.

B. INVESTIGATION OF HIGH TEMPERATURE TEXTURE STRENGTHENING IN α -TITANIUM

Recall that at the temperature of this study, prismatic slip ($\{10\bar{1}0\}$ plane) predominates in the plastic deformation of α -titanium.

Normal fabrication processes produce a strong texture in HCP metals. When titanium is cold-rolled into sheet, then annealed, the deformation and annealing processes have a tendency to align the basal poles $[0001]$ of each grain so that they are predominantly perpendicular to the rolling direction, R.D. [7]. Besides aligning the basal poles, the rolling and annealing also has the tendency to rotate each grain so that the prism pole $[10\bar{1}0]$ coincides with the rolling direction. The ideal recrystallization texture has both the basal pole and the prism poles aligned in the described way, as shown in Figure 3.

The texture attained by cross-rolling several times, then annealing, is a two-dimensional extension of the one-dimensional sheet rolling. In cross-rolling, there is the one rolling direction, but a duplex "ideal" preferred orientation. In the ideal case, the number of grains having their basal poles mutually perpendicular is equal, and all grains have basal poles perpendicular to the rolling direction.

Longitudinal samples are those samples whose loading direction is the same as the rolling direction. If these samples were ideally textured, all basal slip systems and a third of the $\{10\bar{1}0\}$ prismatic systems would be inactive because the resolved shear stress, using Schmid's Law, on these systems is zero. Plastic deformation could readily be accomplished however, because most of the primary slip systems, the $\{10\bar{1}0\} \langle 11\bar{2}0 \rangle$ prismatic systems, are favorably oriented.

On the other hand, transverse samples are those samples whose loading direction is perpendicular to the rolling direction. In these samples all of the basal slip systems will be inactive as in the longitudinal samples. The difference between the transverse and longitudinal samples is that in the transverse samples only half as many primary $\{10\bar{1}0\}$ slip planes will be favorably oriented for slip, see Figure 4.

With fewer primary slip systems available for deformation, the transverse samples should be stronger and more resistant to plastic deformation.

Logic such as given above has been applied technologically to strengthening of HCP metals at ambient temperatures, but not at elevated temperatures. This investigation considers the effectiveness of texture strengthening α -titanium at high temperatures, where the mechanism controlling the deformation rate is generally accepted to be solid-state diffusion [8].

III. EXPERIMENTAL PROCEDURE

A. EQUIPMENT DESCRIPTION AND SAMPLE PREPARATION

All tests were conducted on an Instron Model TT-D floor model testing machine, see Figure 5. This machine is capable of recording loads from 0 to 89,000 newtons and running at cross-head speeds of .00508cm per minute to 50.8cm per minute. (Cross-head speeds can be further reduced by a special technique described later.)

The compression test rig, adapted from an original design by Drs. C. Young and D. Bly, Stanford University, was designed to be compatible with the Instron testing machine. The compression assembly (see Figure 6), consists of a 1-inch diameter Haynes 188 punch and a 3-inch O.D. Inconel cylinder, with a 1.010-inch bore. The punch fits inside the test cylinder, and glides on two machined lands inside the cylinder. Both the punch and the cylinder head have machined recesses which accommodate tungsten carbide platens. Specimens are tested on the tungsten carbide platens.

Temperature control was provided by a Marshall split furnace capable of temperatures in the range of 100 °C-1200°C. Control of the furnace was maintained by a Leeds Northrup Series 60 control unit. Temperature stability of $\pm 3^{\circ}\text{C}$ was attainable.

The atmosphere of the tests was controlled by means of a cylindrical stainless steel sleeve which enclosed the compression test rig and could be evacuated, then back-filled with dry argon.

Water-carrying copper cooling coils were soldered to the top and bottom of the sleeve to protect the vacuum and argon hosing at the top of the sleeve and to protect the polymeric O-ring which provided a seal between the sleeve and the Inconel punch.

The test assembly was evacuated by a General Electric vacuum fore pump. The compression test rig was typically evacuated to 250 millitorr prior to back filling with dry argon.

Chromium-Alumel thermocouples sheathed in 1/16-inch Inconel monitored the temperature. These thermocouples were monitored by a Leeds-Northrup potentiometer.

To increase the capabilities of the machine for slow cross-head speed testing, a synchronous clock motor was used (Figure 7). This clock motor in conjunction with the existing gearing system of the testing machine made the rig capable of cross-head speeds on the order of microns per second.

High purity titanium was obtained from Titanium Metal Corporation of America in the form of 1.27cm-diameter bar, hot rolled at 1400°F from 350g buttons of EL60 electrolytic sponge. The chemical composition of the titanium used in the present investigation is given in Table I.

Crystallographic texture was induced into the titanium by cross-rolling at room temperature the as-received bar down to a .508cm by .518cm cross section. Rolling was done by a Fenn 21cm rolling mill. Such processing corresponded to a 80 percent reduction in cross sectional area.

Transverse and longitudinal samples were machined from the same section of cross rolled titanium bar. Samples were rectangular parallelepipeds with dimensions 0.338cm by 0.338cm by .508cm. Longitudinal samples were prepared with the long dimension corresponding to the rolling direction. Transverse samples were prepared with the long dimension perpendicular to the rolling direction, see Figure 8.

After machining, the specimens were vacuum capsulated in a dynamic vacuum of 5×10^{-6} torr or better in quartz tubing and annealed at 700°C

for over one hour, yielding a grain size of $63\mu\text{m}$ as determined by the mean linear intercept method, see Figure 9.

Over and above the textured specimen, several coarse grain (nearly single crystal) longitudinal right circular cylinder specimen were machined from the extruded bar. After machining, these specimens were vacuum capsulated in a vacuum of 5×10^{-6} torr or better in quartz tubing and annealed at 940°C for 2 hours and 862°C for 40 hours yielding a specimen which was nearly single crystal. The dimension of the right circular cylinders were .200 inches in diameter by .300 inches high.

B. TEST PROCEDURE

The test equipment was brought up to temperature and stabilized before placing a sample in the compression chamber. During this pre-heat, the test chamber was filled with dried argon gas which minimized the oxidation of the compression rig and the tungsten carbide platens. After the rig and test chamber had come up to temperature, a titanium sample was placed between the tungsten carbide platens, the chamber was sealed, and a vacuum of 250 millitorr was drawn on the test chamber. When the vacuum had stabilized the chamber was back-filled with dry argon gas. The process of evacuating and back-filling was then repeated to further purify the atmosphere. A positive pressure of 14kPa was kept in the test chamber during testing so as to maintain atmosphere purity.

Titanium has a great affinity for the gaseous elements hydrogen, carbon, nitrogen, and oxygen, all of which form interstitial solid solutions. These interstitial impurities have a marked strengthening effect on the material. The magnitude of the effect is a strong

function of exposure time and temperature. Testing in the argon atmosphere was therefore necessary to avoid introducing an uncontrolled compositional variable.

After the second back-fill of argon gas the system was allowed to stabilize at a preset temperature, the cross-heads were brought into position, and the test started.

C. METHOD OF DATA TAKING

Twenty-four transverse and 24 longitudinal tests were run on the cross-rolled textured titanium. Eighteen tests were run on coarse grain longitudinal samples. Plots of load (pounds) versus cross-head travel (index) were made for all tests. Tests were run at 6 temperatures ranging from 300°C to 800°C. Cross-head speeds ranged from 1.865×10^{-4} inches/minute to 2×10^{-1} inches/minute. Table II gives a matrix showing the temperatures and cross-head speeds used for the tests.

D. TEXTURE EVALUATION

The x-ray equipment typically used to evaluate crystallographic texture is not available at NPS. The experimental results of Doner and Conrad, and two qualitative techniques were used to estimate the texture developed by our cross-rolling procedure.

1. X-Ray Diffraction

A conventional "pinhole photograph", a modification of the Laue technique for single crystals, was used. This technique applies to an estimate of texture as follows: If the sample is fine-grained and not textured, continuous Debye rings will be photographed. For example, Figure 10 is the pattern obtained from titanium filings using a transmission pinhole technique and Cu K α radiation.

Texture in a sample is indicated by intermittent Debye rings or Debye rings which are formed by spots and are not continuous. If a specimen has a strong texture, crystallographic directions and planes for many grains are spatially aligned. For a given x-ray wavelength, only a few of these grains will have crystallographic planes correctly oriented to diffract. Those similar planes which do, will diffract in the same direction producing a spot on the film. How intermittent or "spotty" the Debye rings appear on the film is an indication of the degree of texture in the sample.

2. Texture Determined by Polarized Light Microscopy

The polarized light microscope provides another means of qualitatively describing the texture of the cross-rolled specimens. The sample is viewed looking along the rolling direction under polarized light with the analyzer crossed with the polarizer. Couling and Pearsall [9], found that when HCP grains were viewed under compensated polarized light, with the analyzer crossed with the polarizer, the direction made by the basal plane traces on the plane of observation could be correlated with a specific direction in the plane of view. They specifically found that when a grain's basal plane trace was aligned exactly parallel to the plane of polarization in the analyzer, that the grain appeared blue. When the field of view was rotated 90° the grain appeared orange.

To apply this technique to our textured titanium, a longitudinal sample was electro polished (40 volts at 1 amp for 25 sec), and etched (using K roll's etch), and viewed under a polarized light microscope. The sample was viewed along the rolling direction. Sufficient contrast was achieved without compensation, and no compensation plate was used.

E. DATA ANALYSIS

Creep behavior of a material is frequently observed to obey an equation of the form:

$$\dot{\epsilon} = K (\sigma/E)^n \exp[-Q_c/RT] \quad (2)$$

where K and Q_c are constants, n is the stress exponent (≈ 5 for $T > 0.5T_n$), E is the elastic modulus, R is the universal gas constant, and T is temperature in $^{\circ}\text{K}$. Taking the natural log of both sides of (2) and rearranging we have:

$$\ln \dot{\epsilon} = n \ln(\frac{\sigma}{E}) + \text{constant} [T = \text{constant}] \quad (3)$$

It also can be shown that equation (3) can be rearranged so that:

$$\ln \dot{\epsilon} = -\frac{Q_c}{R} \frac{1}{T} + \text{constant} [\sigma/E = \text{constant}] \quad (4)$$

Using equation (3) and (4), the output of load versus cross-head travel from the Instron machine was used to construct plots of true stress (normalized by the elastic modulus [10], versus temperature at constant strain rates. Taking constant values of σ/E , plots of strain rate versus T^{-1} were made. As shown by equation (4) such plots would yield values of $-Q_c/R$. At constant values of T , plots of strain rate versus σ/E were also made. Following equation (3) this plot would yield values of n , a measure of the stress dependence for a given strain rate. By obtaining values of n and Q_c , comparisons could be made for the creep behavior of α -titanium as compared to creep behavior of other similar materials.

IV. RESULTS AND DISCUSSION

A. CREEP BEHAVIOR OF α -TITANIUM

As stated earlier, the creep behavior of a material is frequently observed to obey an equation of the form in equation (2).

$$\dot{\epsilon} = K(\sigma/E)^n \exp[-Q_c/RT] \quad (2)$$

Equation (2) can be rewritten as follows:

$$\ln \dot{\epsilon} = n \ln(\sigma/E) + \text{constant} ; [T = \text{constant}] \quad (3)$$

Figures 11 and 12 show the plots of the family of lines from equation (3) for both longitudinal and transverse samples. These plots show that the value of n varied from 5 to 11.6 for the longitudinal samples and 5 to 16 for the transverse samples. If one makes a phenomenological comparison of creep behavior in many materials at these strain rates, an n value of 4.5 to 5 for temperatures greater than $.5 T_m$ is typical. It is also common for this "5 power law" creep behavior to give way to behavior in which n increases as the temperature of the testing decreases. Note that for the strain rates employed here, the $400^\circ - 600^\circ$ lines do not fit the general trend of the data. This effect has been explained by the dynamic strain aging effect that takes place at that range of strain rates and temperatures [11].

Strain aging is the phenomenon wherein dislocation sources, normally active during the deformation process, are made inactive by the accumulation of solute atoms around dislocations, which then pile up and exert a back stress on their sources. Because solute atoms must diffuse through the lattice to accumulate around dislocations, the aging is a temperature-time dependent function.

In titanium, impurities of carbon, oxygen, nitrogen, and hydrogen form interstitial solutions. In the temperature regime of 400 - 600°C the dynamic interaction between dislocations and diffusing interstitial impurities has a significant effect on mechanical properties [11].

The temperature dependence of high-temperature deformation is expressed by Q_c , the creep activation energy. Rewriting equation (2):

$$\ln \dot{\epsilon} = - \frac{Q_c}{R} \frac{1}{T} + \text{constant} ; [\sigma/E = \text{constant}] \quad (4)$$

This is an equation of a straight line with a slope of $-Q/R$. Figure 13 is a plot of a family of these lines. From the slope of these lines the creep activation energy was obtained.

Activation energies of $\sim 255\text{kJ/mole}$ were obtained for the transverse samples and $\sim 289\text{kJ/mole}$ in the longitudinal samples. The author noted that there was a slight difference in the activation energies between the transverse and longitudinal samples. These activation energies compare quite favorably with the creep activation energy found by Doner and Conrad [4]. One is forced to conclude either that the Libanati self-diffusion data for titanium is not accurate or that some as yet undetected experimental problems preclude a correlation of Q_{sd} and Q_c for titanium.

B. TEXTURE ANALYSIS

Figure 14 is the x-ray diffraction pattern obtained from a textured titanium sample using back-reflection. The intermittent Debye rings indicate that our cross-rolled samples are indeed strongly textured.

Okazaki, and Conrad [12], showed that large amounts of cold work followed by subsequent annealing, textured α -titanium so that the majority of basal poles were aligned perpendicular to the rolling

direction of maximum strain with the $\langle 10\bar{1}0 \rangle$ directions making ± 15 deg with the direction of maximum strain.

Figure 15 (a) is a photomicrograph of one of the textured titanium samples, photographed on a plane perpendicular to the rolling direction, under polarized light with the polarizer crossed with the analyzer. The darker (blue) colored grains (grain "B" for example) have the traces of their basal planes exactly aligned with the vertical direction on the photograph, indicating that our texturing procedure oriented the basal poles to positions perpendicular to the rolling direction, a result which would be consistent with the results of Okazaki [12]. Figure 15(b) is a picture of the same grains after a 90° rotation. Note that the dark (blue) grains become light (orange) and light grains become dark upon a 90° rotation. This complete reversal of contrast could only occur in material possessing the duplex crystallographic texture hypothesized earlier and depicted in Figure 4.

The author noted a difference in sample deformation between transverse and longitudinal samples. Longitudinal samples displayed a very regular deformation with all four sides of the specimen expanding out uniformly as deformation took place. Uniform deformation of longitudinal samples could occur because equal numbers of grains had components of their primary $\langle 11\bar{2}0 \rangle$ slip directions oriented perpendicular to each specimen side. The transverse samples, however, deformed non-uniformly; specimens originally square in cross-section became rectangular in cross-section. This non-uniform deformation can be rationalized by recalling the sample texture; because the $\langle 11\bar{2}0 \rangle$ slip directions on the most active slip systems (prismatic) had components perpendicular to only one pair of the sample sides, the strain in that transverse direction

far exceeded that in the other transverse dimension. The author believes that the non-uniform deformation observed in transverse specimens lends considerable credence to the hypothesis that prismatic slip in transverse samples was limited because of preferred orientation.

C. TEXTURE STRENGTHENING

Plots of stress versus temperature at constant strain rates showed the consistent difference in deformation strength between longitudinal and transverse samples, see Figures 16-19.

At the higher strain rates employed ($1.66 \times 10^{-2} \text{ sec}^{-1}$) and ($1.66 \times 10^{-3} \text{ sec}^{-1}$) the degree of texture strengthening was found to be relatively constant. The slight deviations from smooth curves manifest the strain aging produced by impurities. This effect has been consistently observed by others [4 and 11]. The flow stress, at 10 percent strain, for the transverse samples averaged 16MPa higher than the flow stress for longitudinal samples.

For the two slower strain rates ($1.66 \times 10^{-4} \text{ sec}^{-1}$ and $1.54 \times 10^{-5} \text{ sec}^{-1}$) the curves can be crudely viewed as two temperature regimes, $> 550^\circ\text{C}$ and $< 550^\circ\text{C}$. Below $\sim 550^\circ\text{C}$, there is a very large difference between the flow stress of transverse and longitudinal samples. At 300°C , $\dot{\epsilon} = 1.54 \times 10^{-5} \text{ sec}^{-1}$, the difference in flow stress is 44MPa, a 30% increase in strength for the transverse sample. At $T \geq 550^\circ\text{C}$ the texture strengthening effect, though clearly evident, was less important. Transverse samples were ~ 5 percent stronger than the longitudinal samples.

In fact, Figures 19-20, show that as the strain rate approaches the commonly observed creep rates (10^{-6} sec^{-1}) texture strengthening at the most useful temperatures for titanium alloys ($300^\circ\text{--}500^\circ\text{C}$)

becomes quite important. Differences in flow stresses ranging from 30% to 48% were observed.

Curves for coarse grain (grain size $\sim .5\text{cm}$) samples are included on the plots of the three higher strain rates ($1.66 \times 10^{-4} \text{ sec}^{-1}$ through $1.66 \times 10^{-2} \text{ sec}^{-1}$). These samples were consistently weaker than the textured samples. This result is as expected in view of the very large grain size observed in the coarse-grained samples. Figures 17-19 show that reducing grain size significantly strengthens titanium particularly at moderate-to-high strain rates and moderate temperatures.

V. CONCLUSIONS

The results conclude that there is a high potential for high temperature texture strengthening in α -Ti. At strain rates very near the commonly observed creep rates, and at the most useful temperatures for titanium alloys, differences in flow stresses ranging from 30 percent to 48 percent were observed.

There as yet may be undetected experimental problems precluding a correlation of Q_{sd} and Q_c . For this investigation Q_c did not follow the correlation depicted in Figure 2. Rather Q_c was found to be 80 percent greater than the Q_{sd} found by Libanati [5] but was in accord with Q_c found by Doner and Conrad [4].

Qualitatively it may be concluded that during deformation basal poles in HCP materials do align perpendicular to the direction of maximum strain.

TABLE I

*
CHEMICAL COMPOSITION OF TITANIUM USED IN TESTS, wt. pct.

	O	N	H	C	Cl	Fe	Si	Mg
Maximum	0.020	< 0.002	0.005	0.012	0.040	< 0.001	< 0.004	< 0.001
Typical	0.010	< 0.002	0.003	< 0.009	0.080	< 0.001	< 0.002	< 0.001
							Mn	H ₂ O
							< 0.001	< 0.012
							< 0.001	< 0.010

* Analysis by Titanium Metals Corporation of America

TABLE II
MATRIX OF CROSS-HEAD SPEEDS
TEMPERATURES USED

Temperature, °C	Cross-Head Speed $\frac{\text{cm}}{\text{min}}$			
	.000475	.00508	.0508	.508
300	L/T	L/T/2C	L/T/2C	L/T/2C
400	L/T	L/T	L/T	L/T
500	L/T	L/T/2C	L/T/2C	L/T/2C
600	L/T	L/T	L/T	L/T
700	L/T	L/T/2C	L/T/2C	L/T/2C
800	L/T	L/T	L/T	L/T

L - one longitudinal test
T - one transverse test
C - one coarse grain test

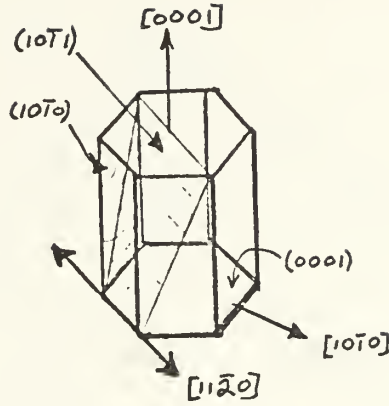


Fig. 1. HCP Unit cell with principal planes and directions indicated.

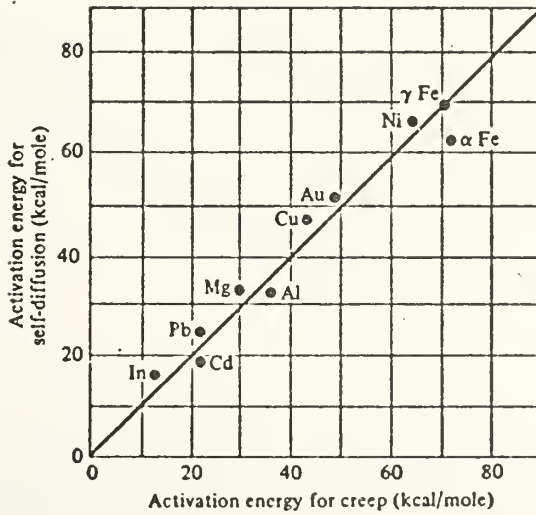


Fig. 2. Comparison of the activation energies for creep and self-diffusion of several materials. (J. E. Dorn, in "Creep and Recovery", American Society for Metals, 1957, p. 255).

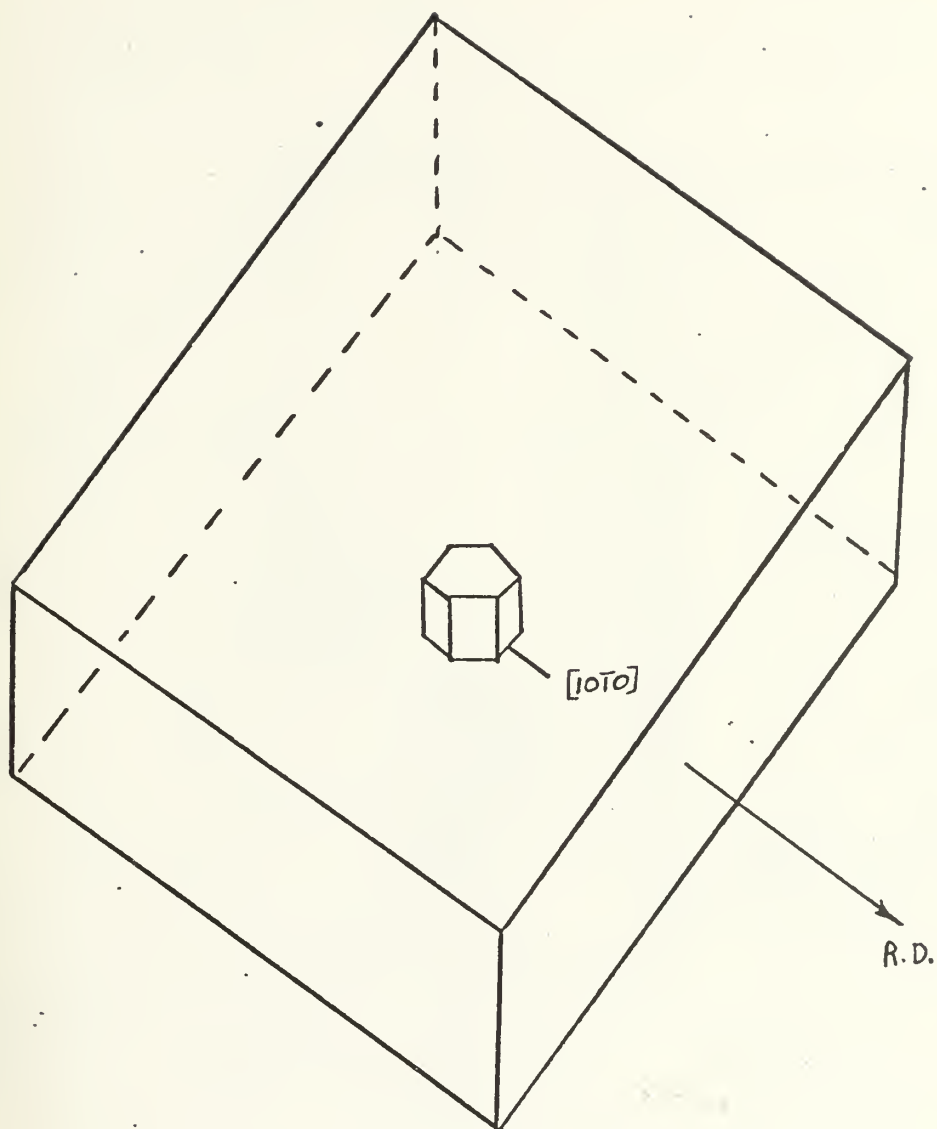


Fig. 3. Ideal recrystallization texture in titanium sheet; Basal $[0001]$ poles are perpendicular to R.D. and the $[10\bar{1}0]$ direction is parallel to R.D.

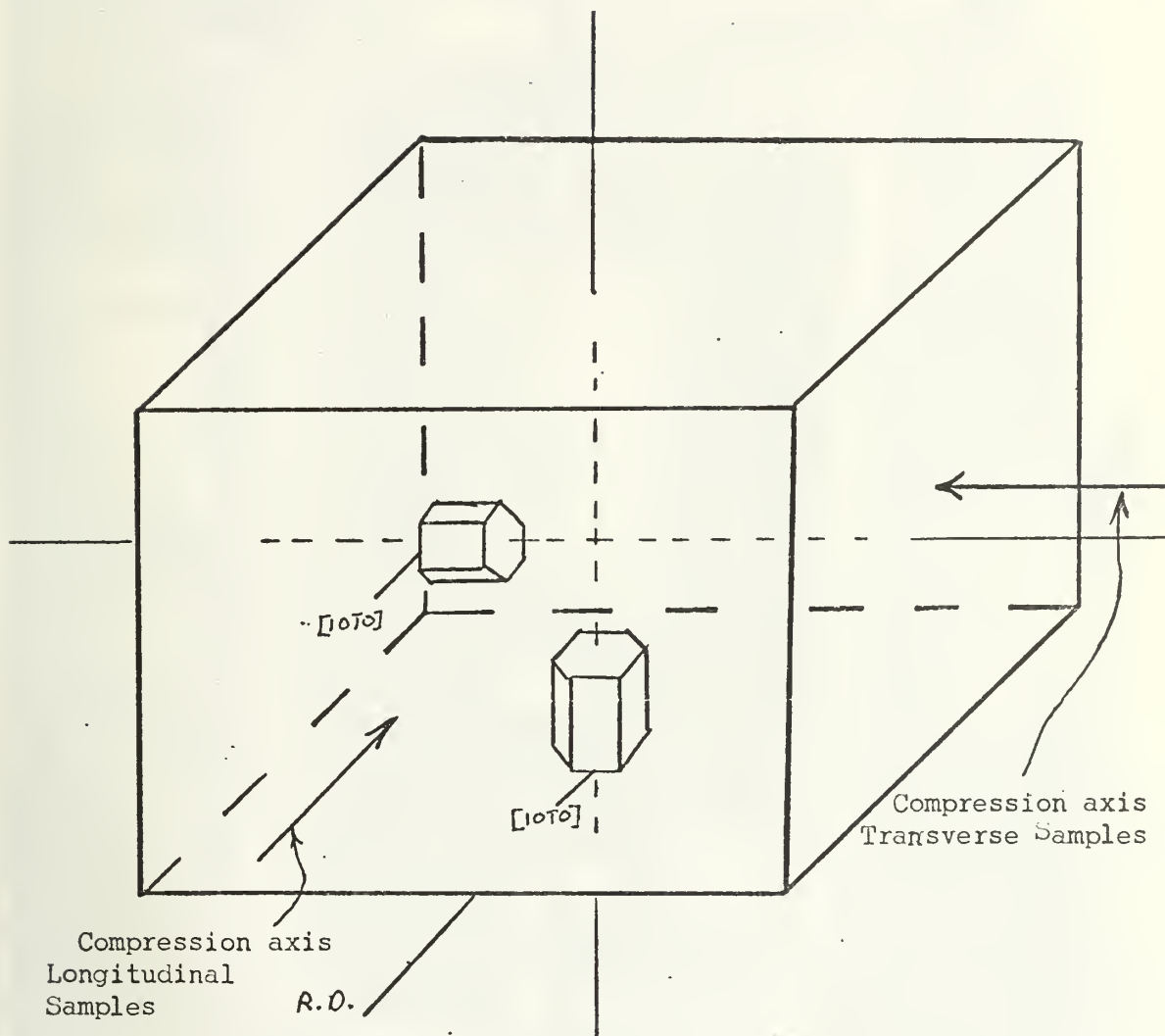


Fig. 4. Ideal duplex recrystallization texture in cross-rolled and annealed α -titanium. Equal numbers of grains occupy each of the orientations depicted.

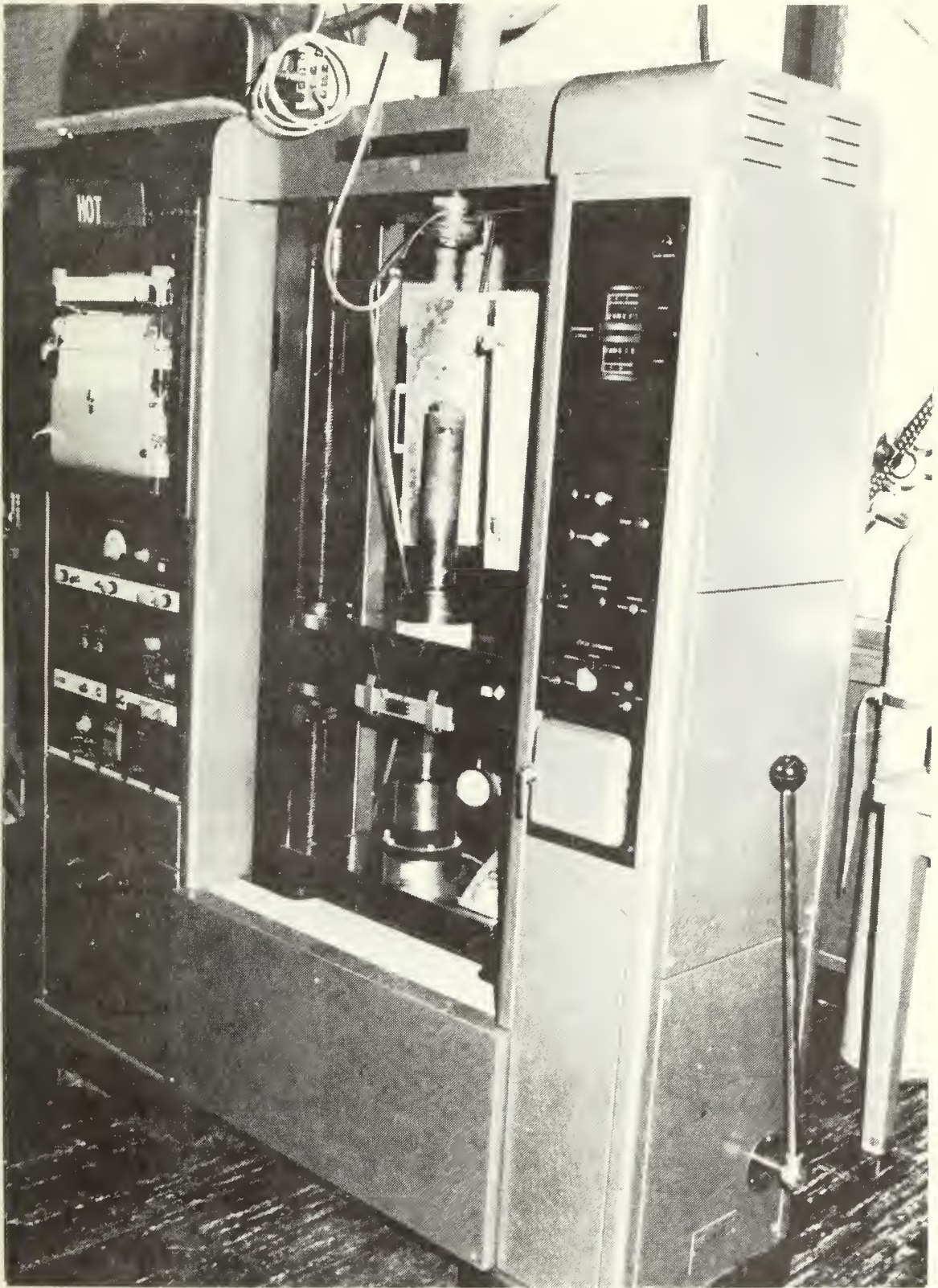


Fig. 5. Instron Model TT-D testing machine with compression rig.

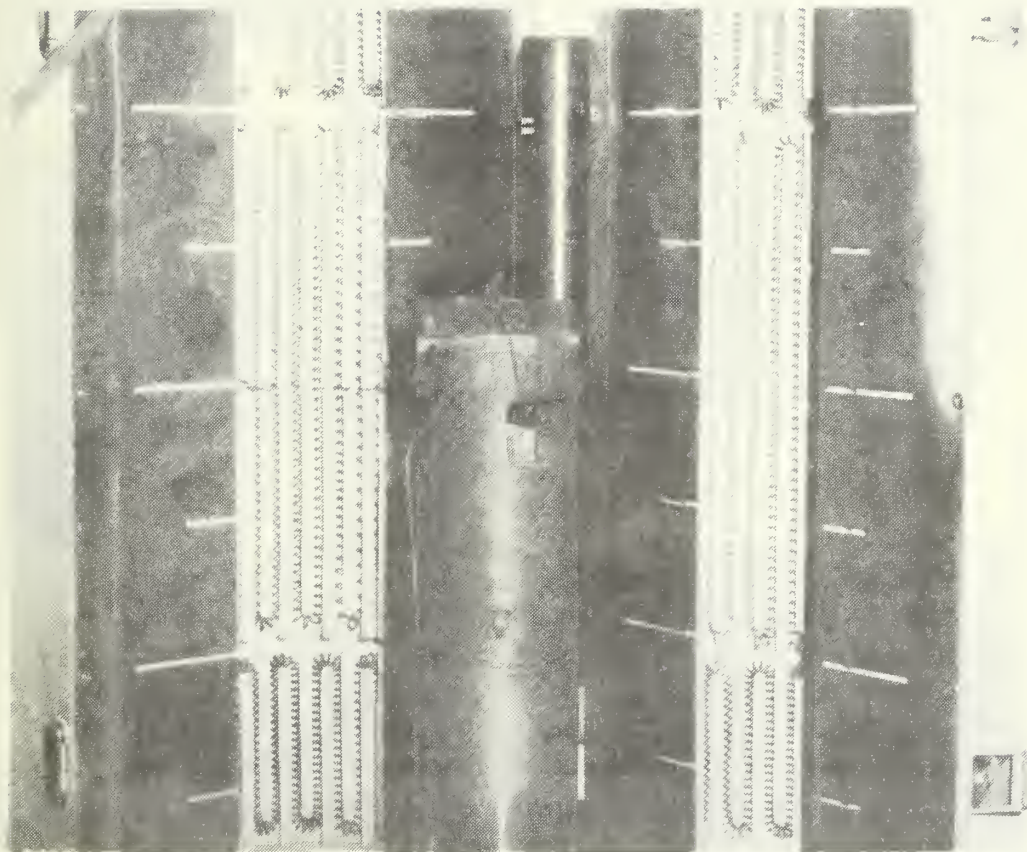


Fig. 6. Compression rig with Marshall Furnace.

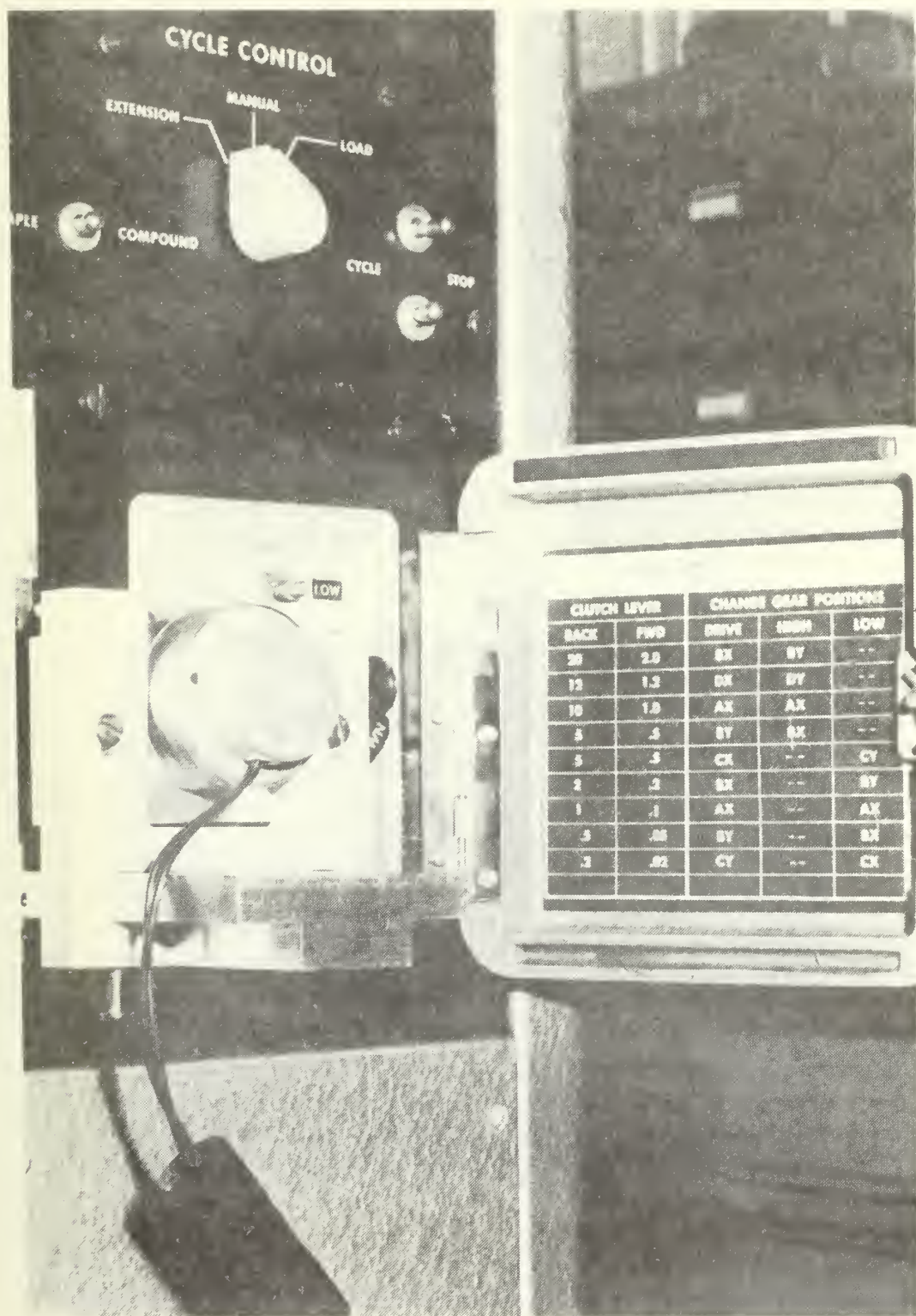


Fig. 7. Synchronous motor on Instron machine; used for slowest strain rate.

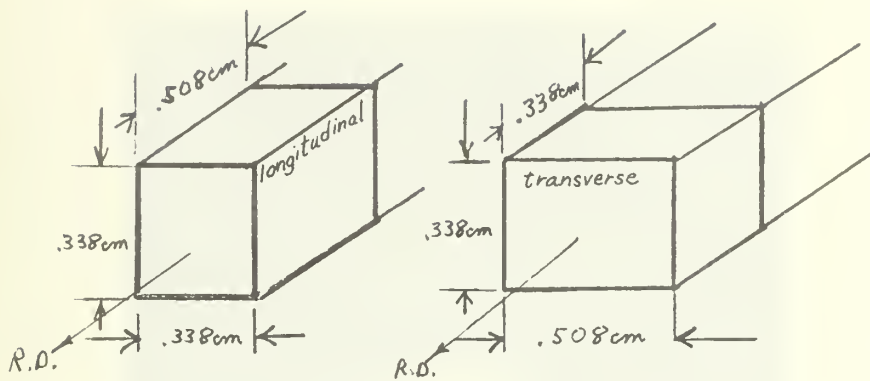


Fig. 8. Longitudinal and transverse samples sectioned from cross-rolled bar.

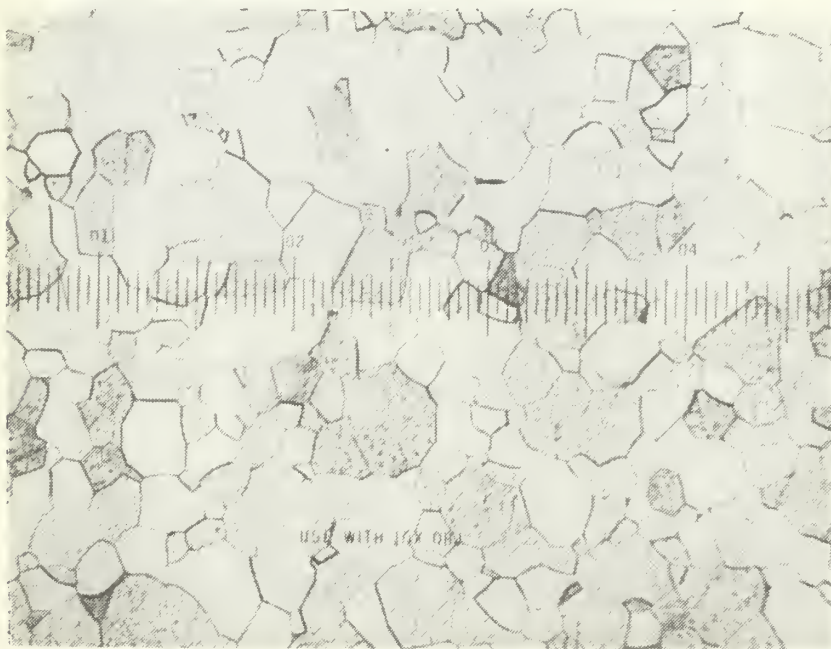


Fig. 9. View of grain structure of textured sample 100X.



Fig. 10. X-ray diffraction pattern obtained from titanium filings.

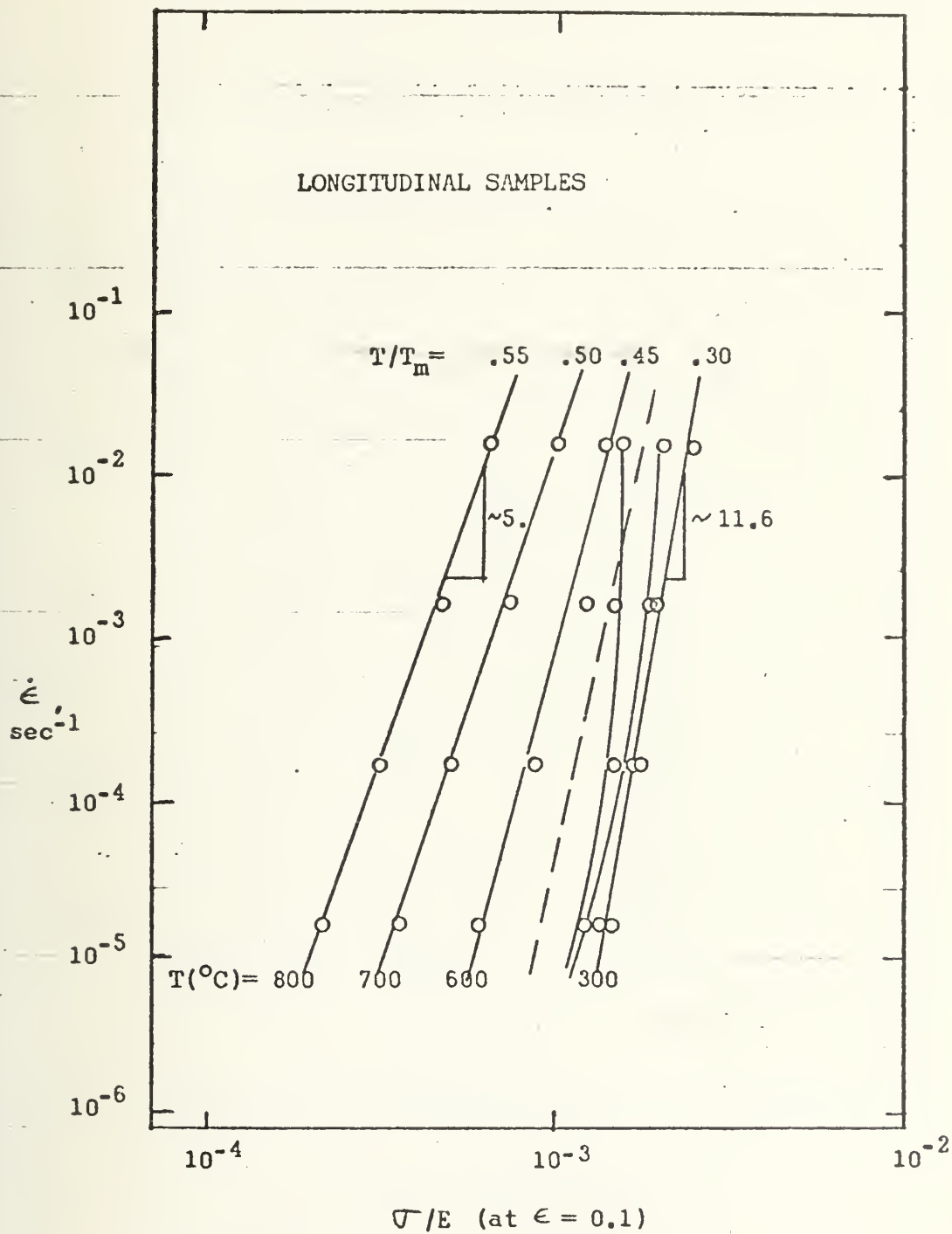


Fig. 11. Plot of strain rate versus normalized flow stress at constant temperature; Longitudinal samples of cross-rolled α -titanium.

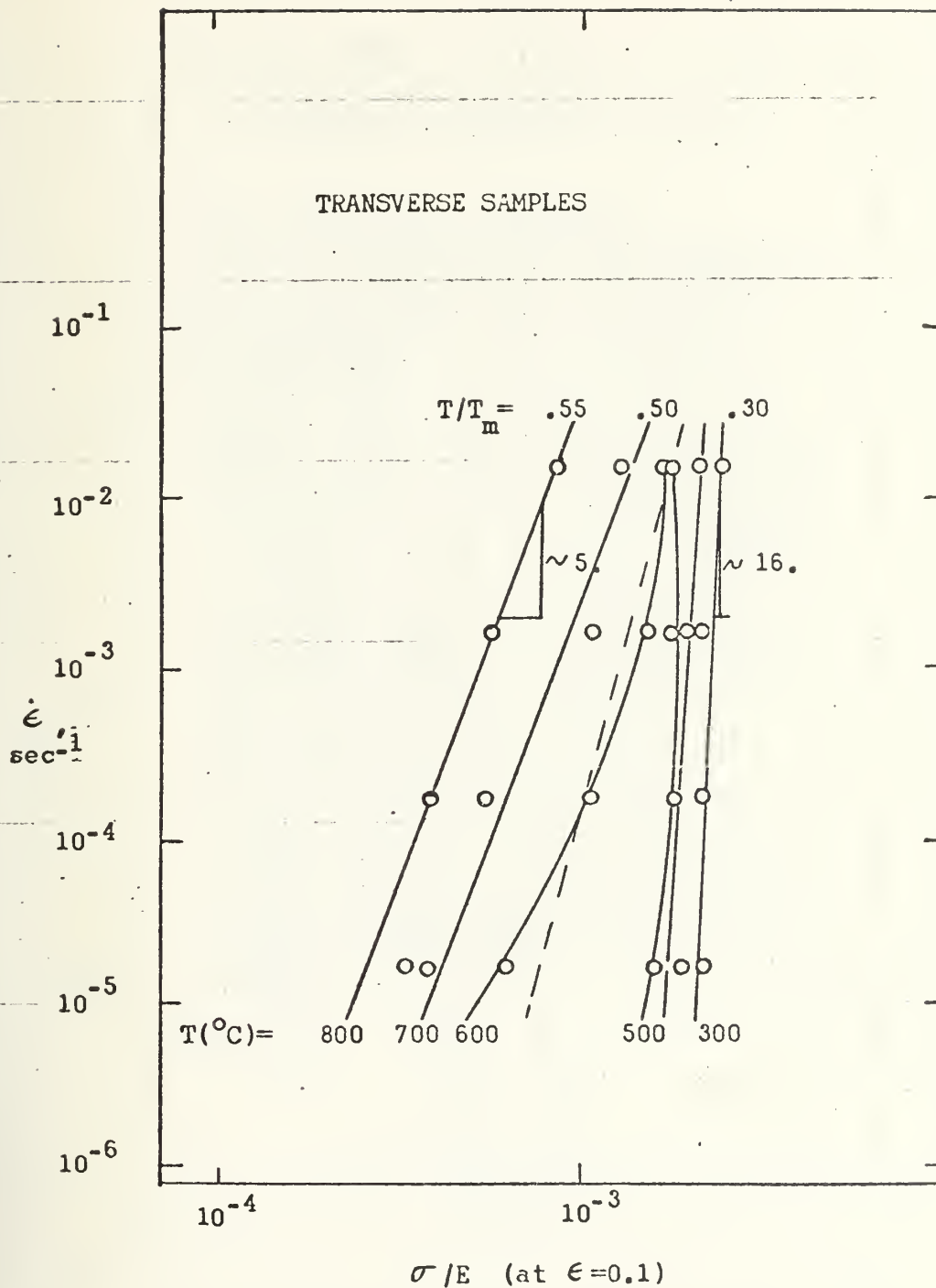


Fig. 12. Plot of strain rate versus normalized flow stress at constant temperature; Transverse samples of cross-rolled α -titanium.

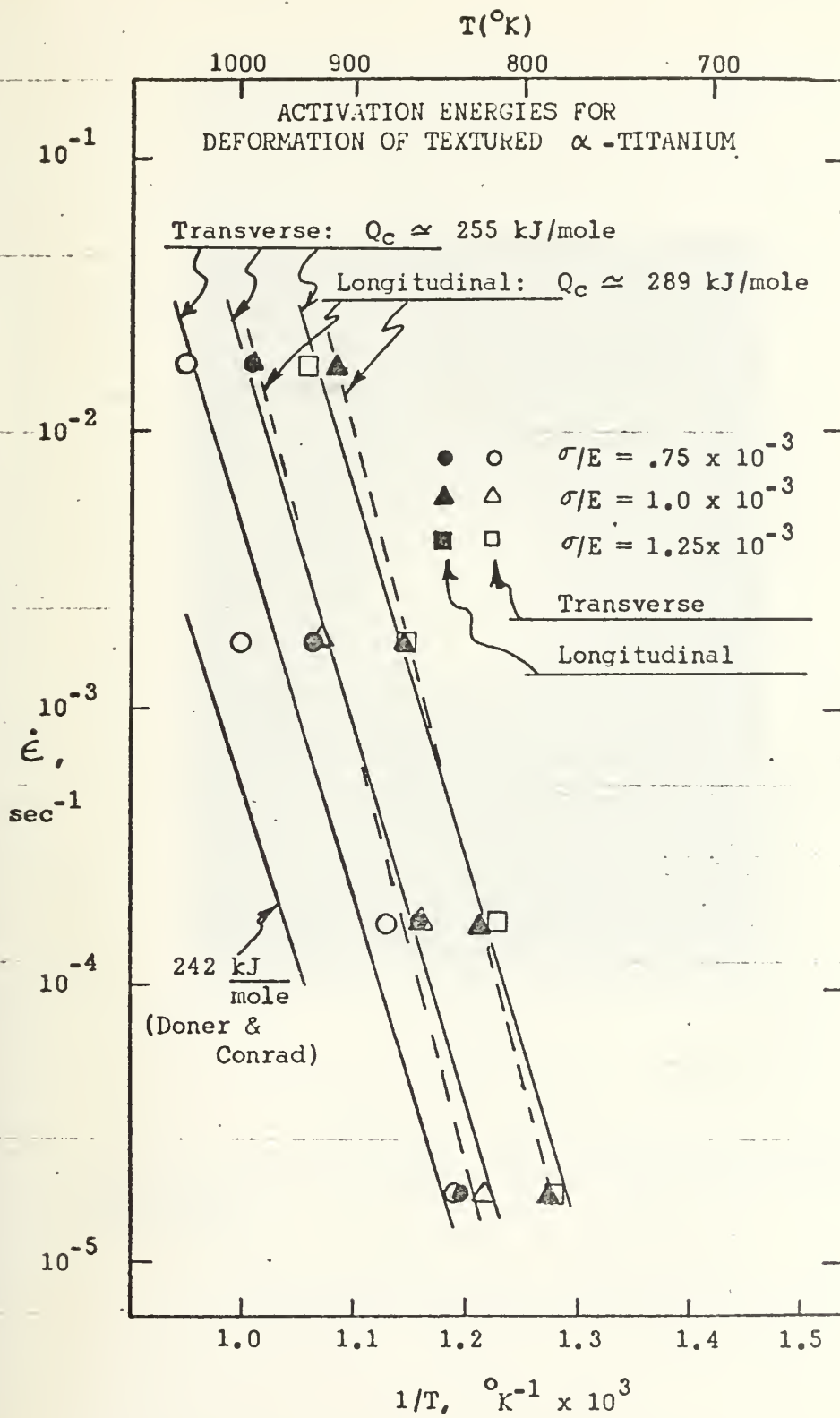


Fig. 13. Plot of strain rate versus inverse of temperature at constant σ/E .

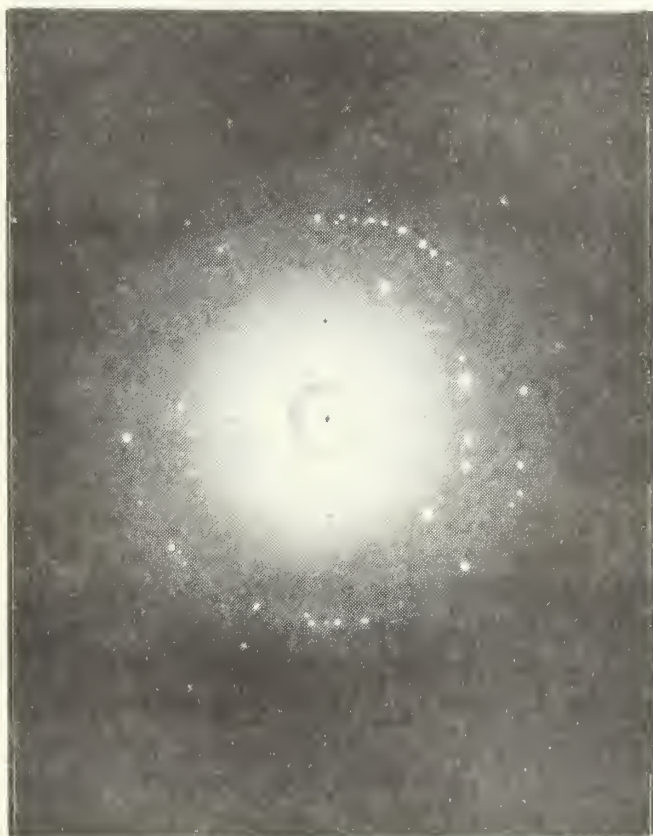
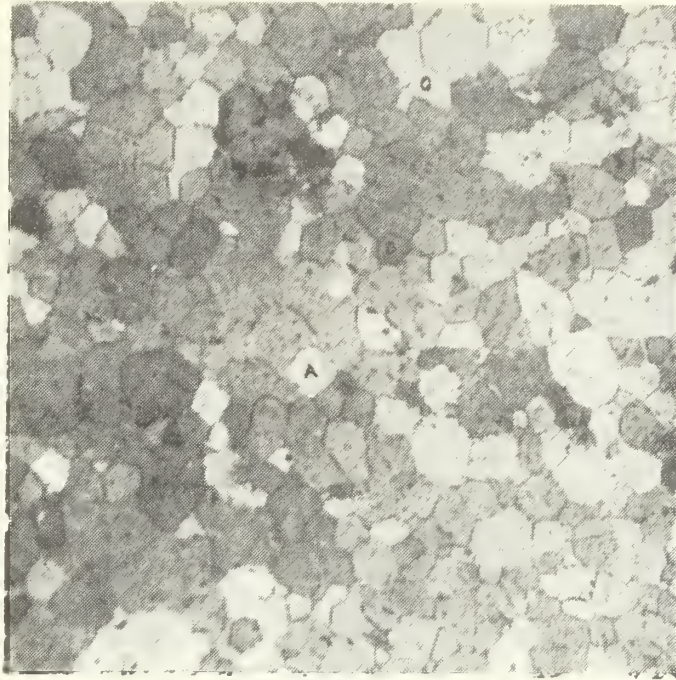
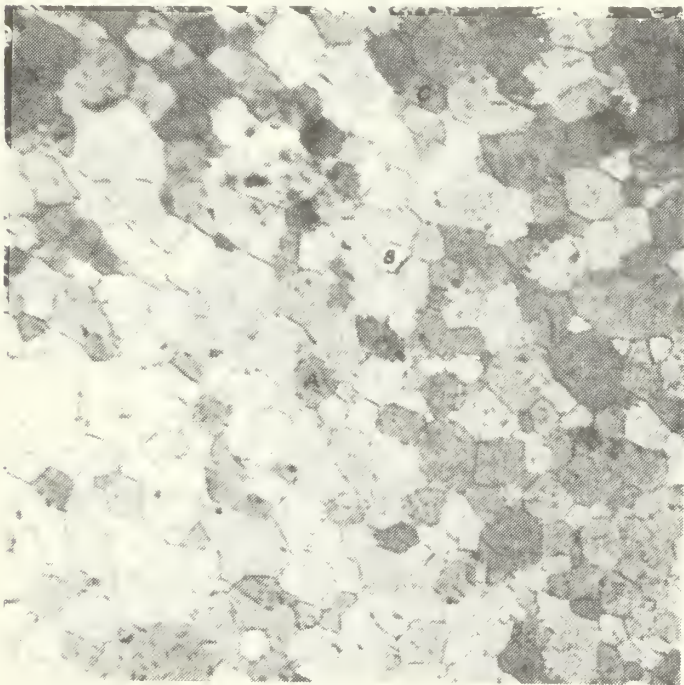


Fig. 14. X-ray diffraction pattern obtained from textured titanium sample.



(a)



(b)

Fig. 15. Photo-micrograph of textured α -titanium sample under polarized light; Plane view is perpendicular to R.D. (a) grains in original orientation. (b) grains after 90° Rotation.

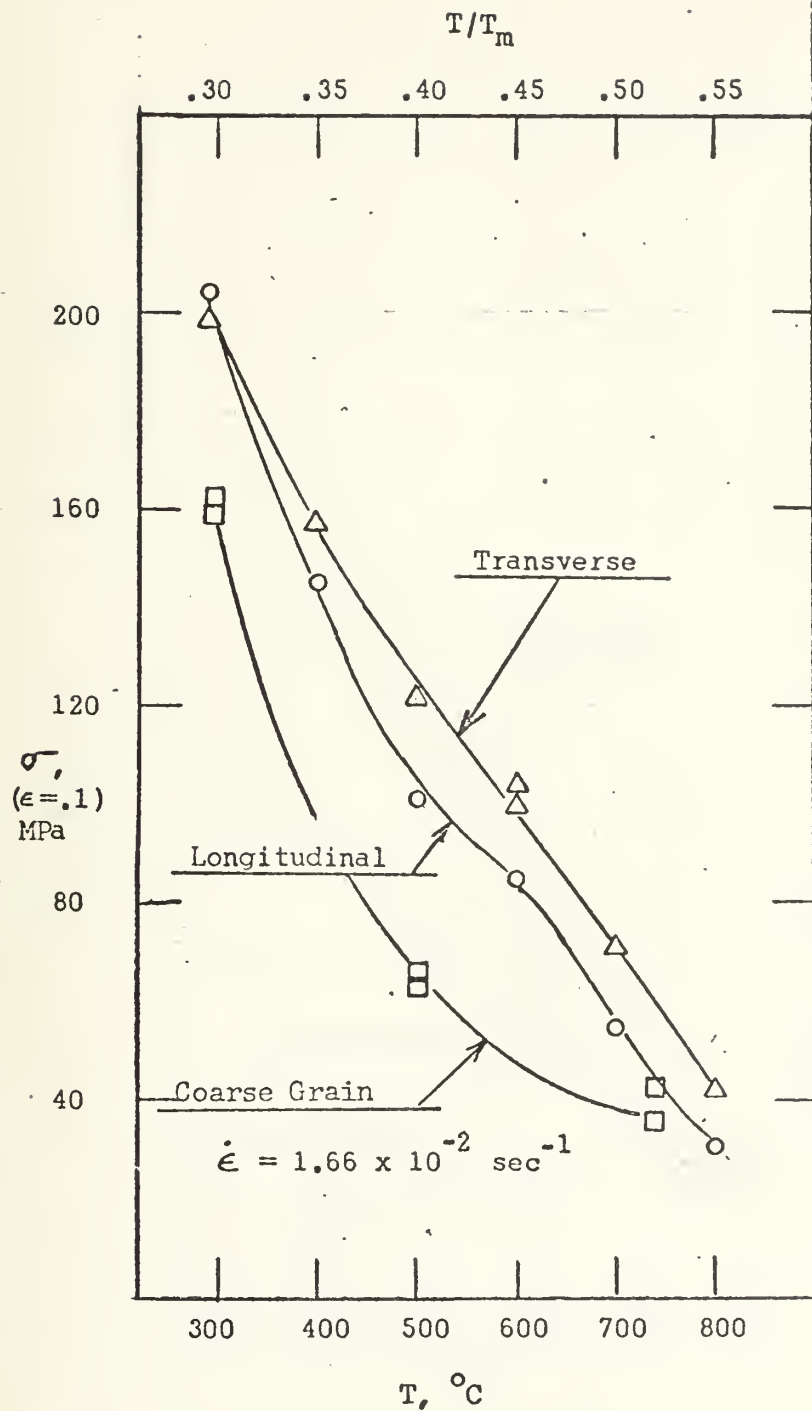


Fig. 16. Plot of flow stress at 10% strain versus temperature for textured α -titanium; $\dot{\epsilon} = 1.66 \times 10^{-2} \text{ sec}^{-1}$.

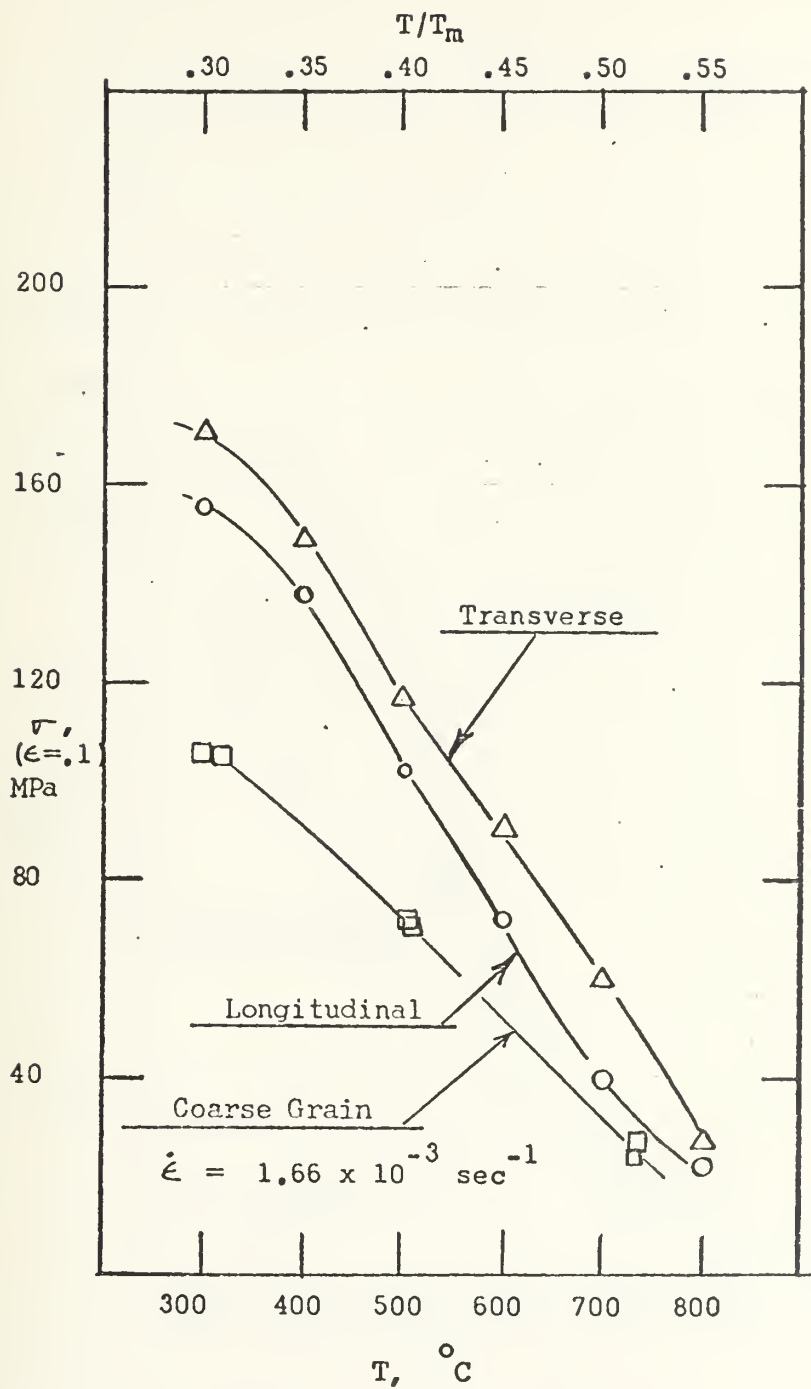


Fig. 17. Plot of flow stress at 10% strain versus temperature for textured α -titanium; $\dot{\epsilon} = 1.66 \times 10^{-3} \text{ sec}^{-1}$.

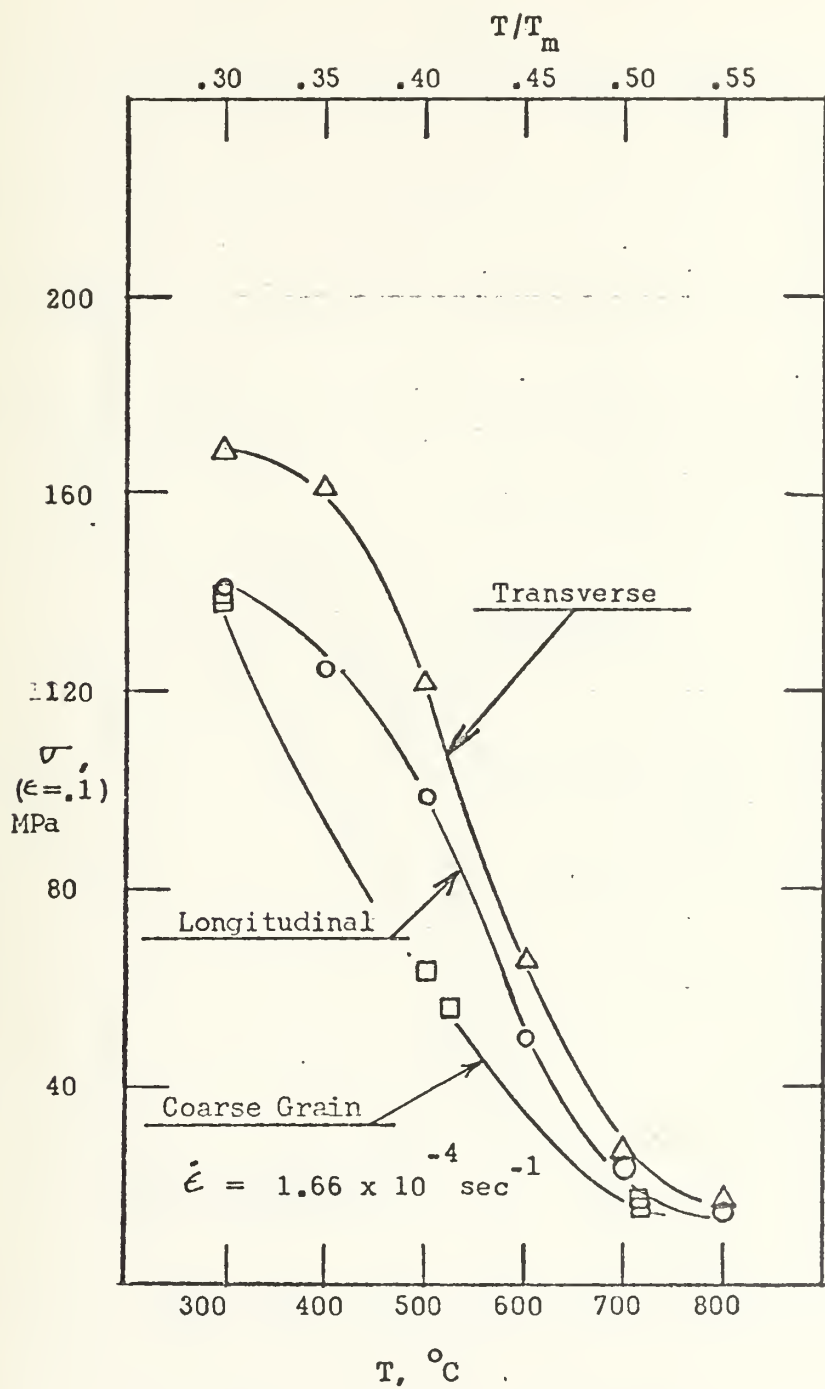


Fig. 18. Plot of flow stress at 10% strain versus temperature for textured α -titanium; $\dot{\epsilon} = 1.66 \times 10^{-4} \text{ sec}^{-1}$.

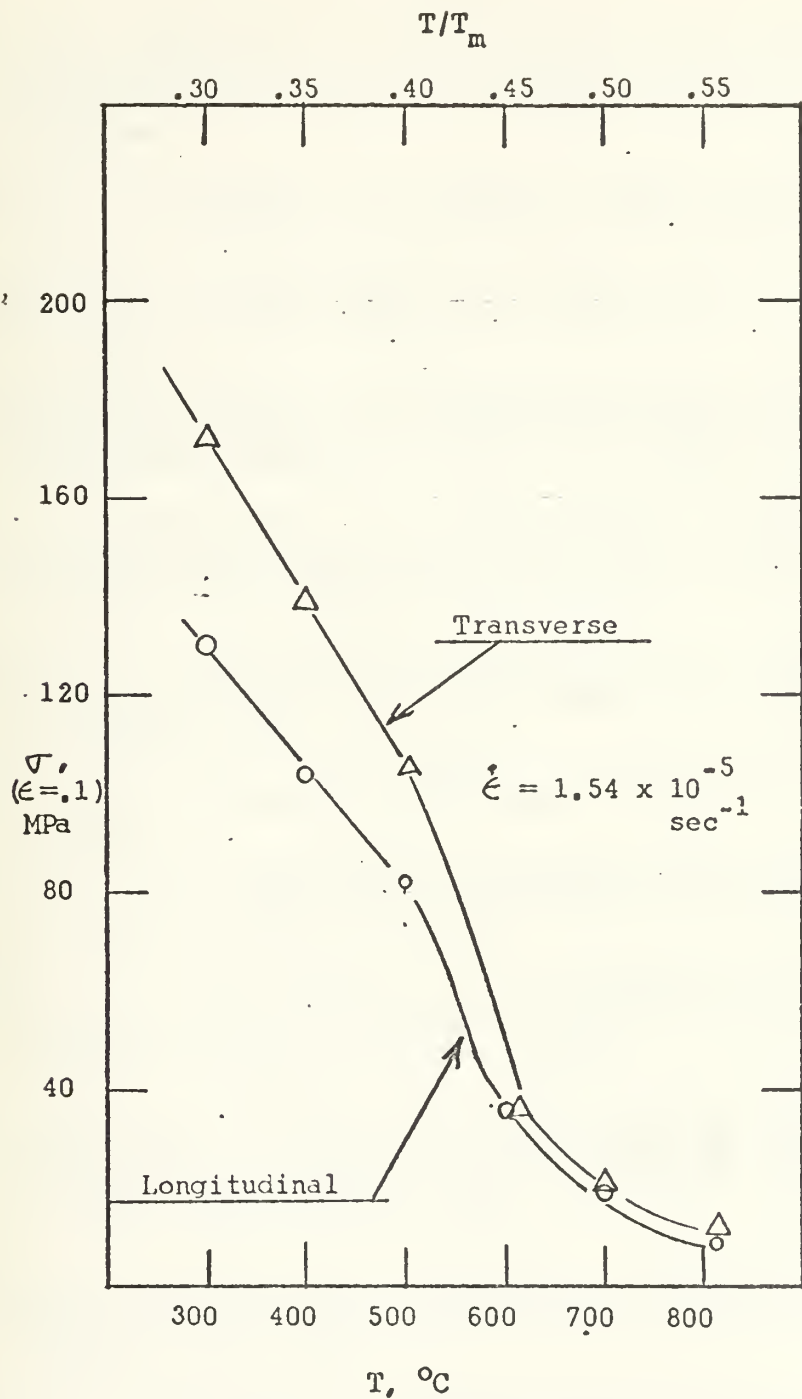


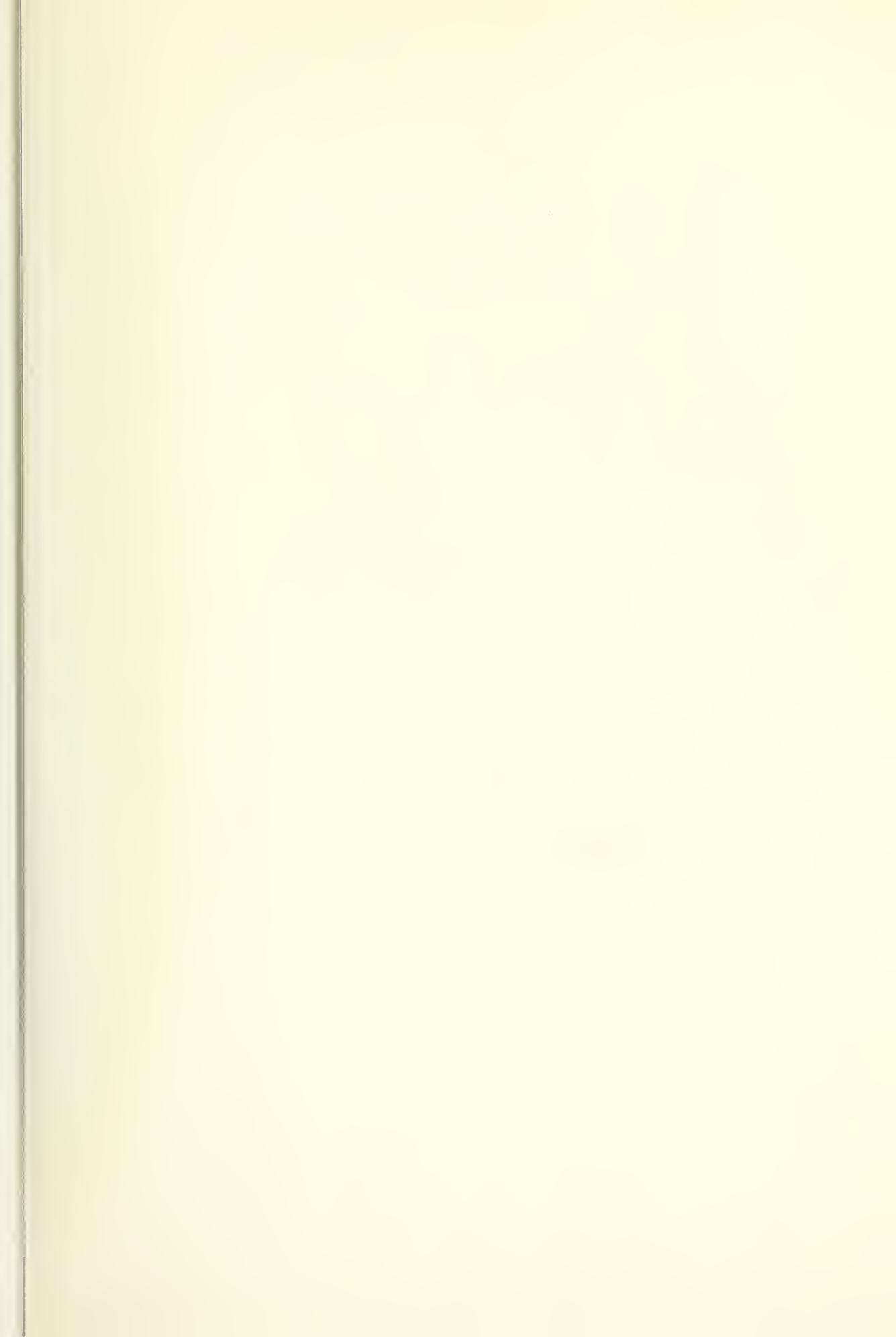
Fig. 19. Plot of flow stress at 10% strain versus temperature for textured α -titanium; $\dot{\epsilon} = 1.54 \times 10^{-5} \text{ sec}^{-1}$.

REFERENCES

1. Doyle, J.r., Ruckle, D. L., and S. Prague, "High Strength Titanium Alloys for Aircraft Gas Turbine Applications," paper from Proceedings of the Science, Technology and Application of Titanium Symposium.
2. Jahnke, L.P., "Titanium in Jet Engines," paper from Proceedings of the Science, Technology, and Application of Titanium Symposium.
3. Vorobev, Gorin, and Khoroshun, Izest. Akad. Nauk, SSSR, Metally, May-June 1971, (3), 181-182.
4. Doner, M. and Conrad, H., "Deformation Mechanisms in Commercial Ti-50A (0.5 at. pct. Oeg) at Intermediate and High Temperatures (0.3-0.6T_m)" Metallurgical Transactions, Vol. 4, p. 2809, Dec. 1973.
5. Dymant, F. and Libanati, C.M., "Self-Diffusion of Ti, Zr, and Hf in Their HCP Phases, and Diffusion of Nb⁹⁵ in HCP Zr," Journal of Materials Science, Vol. 2, p. 349, 1968.
6. Edwards, G. R., McNelley, T.R., and Sherby, O.D., "High Temperature Texture Strengthening in Zinc," Scripta Metallurgica, Vol. 8, pp. 475-480, 1974.
7. Backofen, W.A., Deformation Processing, Addison-Wesley Publishing, Co., 1972.
8. Eisenstadt, M.M., Introduction to Mechanical Properties of Metals, Macmillan Co., New York, 1971.
9. Couling, S. L., and Pearsall, G.W., "Determination of Orientation in Magnesium by Polarized Light Examination, Transactions AIME," Journal of Metals, July 1957, p. 939.
10. Armstrong, P.E., and Brown, H.L., "Dynamic Young's Modulus Measurements above 1000°C on Some Pure Polycrystalline Metals and Commercial Graphites," Transactions of the Metallurgical Society of AIME, vol. 230, August 1964, p. 962.
11. Garde, A.M., Samthanam, A.T., Reed-Hill, R.E., "The Significance of Dynamic Strain Aging in Titanium," Acta Metallurgica, Vol. 20, February 1972, p. 215.
12. Okazaki K., and Conrad, H., "Recrystallization and Grain Growth in Titanium: One Characterization of the Structure," Metallurgical Transactions, 1972, vol. 3, p. 2411.

DISTRIBUTION LIST

- | | | |
|----|---|---|
| 1. | Defense Documentation Center
Cameron Station
Alexandria, Virginia 22314 | 2 |
| 2. | Library, Code 0212
Naval Postgraduate School
Monterey, California 93940 | 2 |
| 3. | Asst. Professor Glen Edwards (Thesis Advisor)
Code 59Ed
Department of Mechanical Engineering
Naval Postgraduate School
Monterey, California 93940 | 1 |
| 4. | Professor Harry Keith
Department of Mechanical Engineering
United States Naval Academy
Annapolis, Maryland 21412 | 1 |
| 5. | Ensign Robert W. Rolfes, USN (Student)
U.S. Naval Nuclear Power School,
July Class
Mare Island, California 94592 | 1 |



153631

Thesis
R68946
c.1

Rolfes

High-temperature texture strengthening in α -titanium.

30314

JUN 3 85

153631

Thesis
R68946
c.1

Rolfes

High-temperature texture strengthening in α -titanium.

thesR68946

High-temperature texture strengthening i



3 2768 001 98112 9
DUDLEY KNOX LIBRARY